Green Synthesis of Tea Tree Oil–Mediated Iron Oxide Nanoparticles for Efficient Arsenate [As(V)] Removal: Synthesis, Characterization and Adsorption Mechanism

*Sakshi Vashistha, Ekta Bhatt, Pammi Gauba**
[1]Department of Biotechnology, Jaypee Institute of Information Technology, Sector 62, Noida, Uttar Pradesh, 201309, India
Corresponding Author Email: pammi.gauba@mail.jiit.ac.in

Abstract This study describes how iron oxide nanoparticles were made using tea tree oil and tested for their ability to remove arsenate [As(V)] from water. The nanoparticles were examined with several techniques, including FESEM, TEM, XRD, FTIR, zeta potential analysis, and GC–MS, to understand their shape, structure, and surface features. Experiments were conducted to determine how factors such as pH (2 to 7), contact time (0 to 240 minutes), adsorbent amount (0.5 g per liter), and initial As(V) concentration (10 to 100 mg per liter) at 25 °C affected arsenate removal. The best adsorption happened at pH 5. Most of the arsenate was removed in the first 60 minutes, and the process reached a balance at about 240 minutes. The results showed that the pseudo-second-order kinetic model best fit the data ($R^2 \approx 0.998$), indicating that chemisorption is the main process. The Langmuir and the Freundlich isotherm models were used to analyze the equilibrium data. The Langmuir model fit better ($R^2 \approx 0.998$) than the Freundlich model ($R^2 \approx 0.987$), suggesting that adsorption mostly happens in a single layer on similar active sites. The Langmuir model predicted a maximum adsorption capacity of 216.9 mg/g. The mechanism suggests that As(V) is mainly removed via inner-sphere surface complexation, in which arsenate exchanges with surface ≡Fe–OH groups, aided by positive electrostatic interactions in mildly acidic conditions. Overall, iron oxide nanoparticles prepared with tea tree oil exhibit strong adsorption capacity for arsenate, making them promising for sustainable arsenic removal.

Keywords: Arsenate removal, Batch adsorption, Green synthesis, Iron oxide nanoparticles, Langmuir isotherm, Tea tree oil

1. Introduction

Arsenic contamination of groundwater remains a critical global environmental and public health concern. Naturally occurring geogenic processes, mining activities, and industrial effluents contribute to elevated arsenic levels in drinking water sources. The World Health Organization (WHO) has established a maximum permissible limit of 10 μg L^{-1} (0.01 mg L^{-1}) for arsenic in drinking water due to its carcinogenicity and association with skin, lung, bladder, and liver cancers, as well as cardiovascular and neurological disorders [1]. However, arsenic concentrations exceeding 50–300 μg L^{-1} have been widely reported in contaminated regions of South and Southeast Asia, including India and Bangladesh [2]. These levels exceed international safety standards, necessitating efficient, cost-effective remediation strategies.

Adsorption is a popular method for treating contaminated water because it is simple to use, effective at removing oxyanion pollutants, and affordable. Iron oxide nanomaterials are particularly effective at removing As(V) because they bind strongly to arsenate via their Fe–OH groups. Arsenate sticks to iron oxides mainly through electrostatic attraction and by forming specific chemical bonds, and this process depends on factors like the solution's pH, the surface charge (pH_{pzc}), and the number of surface hydroxyl groups [3, 4]. The adsorption rate is often described by pseudo-second-order models, while the amount adsorbed at equilibrium usually fits either the Langmuir or the Freundlich isotherm, depending on the surface properties. Chemically synthesized iron oxide nanoparticles can adsorb large amounts of arsenic, but traditional production methods often use synthetic chemicals that may harm the environment or pose safety risks. As a result, greener methods that use plant extracts and essential oils have become attractive alternatives. Compounds like terpenoids, phenolics, and alcohols from plants help reduce and stabilize nanoparticles during their formation, and they also add surface groups that can improve how well the nanoparticles adsorb arsenic [5]. Tea tree oil (Melaleuca alternifolia) is rich in terpenes like terpinen-4-ol, γ-terpinene, and other oxygenated monoterpenes, which can bind to metal ions and help stabilize nanoparticle surfaces [6]. Although more researchers are exploring the use of essential oils to produce nanoparticles, there are still few detailed studies on the use of tea tree oil–based iron oxide nanoparticles to remove arsenate. This study synthesizes iron oxide nanoparticles using tea tree oil as a green reducing and stabilizing agent and evaluates their effectiveness in removing As(V) from aqueous solutions. The nanoparticles were characterized by X-ray diffraction (XRD), Fourier-transform infrared spectroscopy (FTIR), scanning electron microscopy (FeSEM), Transmission Electron Microscopy (TEM), GC-MS and Zeta Potential to elucidate structural and surface properties. Batch adsorption experiments assessed the effects of contact time (up to 240 minutes), adsorbent dose, solution pH, initial arsenate concentration, and temperature. Adsorption kinetics and equilibrium data were analysed using

established models to clarify the adsorption mechanism. The present study provides a preliminary evaluation of arsenic removal using tea tree oil-derived iron oxide nanoparticles through batch adsorption experiments.

2. Materials and Methods

2.1 Chemicals and Reagents

Ferric chloride hexahydrate ($FeCl_3 \cdot 6H_2O$, ≥98%) served as the iron precursor for nanoparticle synthesis. Commercial tea tree oil (Melaleuca alternifolia), obtained by steam distillation, functioned as the green reducing and stabilizing agent. Tween 20 (polyoxyethylene sorbitan monolaurate) acted as a non-ionic surfactant to facilitate the emulsification of tea tree oil in an aqueous medium. Absolute ethanol (≥99.9%) was utilized as a cosolvent to enhance miscibility between the organic and aqueous phases. Sodium hydroxide (NaOH, ≥98%) was applied to adjust the pH during nanoparticle formation. All chemicals were of analytical grade and used without further purification. Deionized (DI) water was employed throughout the experiments.

2.2 Synthesis of Iron Oxide Nanoparticles

Iron oxide nanoparticles were synthesized via alkaline precipitation, with tea tree oil as an environmentally friendly stabilizing agent. A mixture of 2 mL Tween 20, 3 mL absolute ethanol, and 10 mL tea tree oil was magnetically stirred at 680 rpm for 30–35 minutes to form a homogeneous emulsion. Separately, 162 mg of $FeCl_3 \cdot 6H_2O$ was dissolved in 100 mL of deionized water under continuous stirring at room temperature. The ferric chloride solution was added dropwise to the oil–surfactant mixture under vigorous stirring. Subsequently, 1 M NaOH solution was introduced gradually until the reaction mixture reached a pH of approximately 10–11. The alkaline environment promoted the hydrolysis of Fe^{3+} ions and the formation of iron hydroxide nuclei, which subsequently transformed into iron oxide nanoparticles during aging. The reaction mixture was stirred for an additional 30–40 minutes and then aged at room temperature for 72 hours to ensure complete particle growth and stabilization by tea tree oil components. The resulting precipitate was separated by centrifugation at 6000 rpm for 15 minutes, washed repeatedly with deionized water and ethanol to remove residual surfactant and unreacted species, and dried at 60 °C for 12 hours. The dried product was ground into a fine powder and stored for subsequent characterization and adsorption studies [5, 7].

3. Characterization of Materials

The structural, morphological, and surface properties of synthesized iron oxide nanoparticles (IONPs) were evaluated using a range of analytical techniques. Field emission scanning electron microscopy (FE-SEM) was used to examine surface morphology and particle aggregation (Central Research Facility, IIT Delhi) (ZEISS EVO 18). Transmission electron microscopy (TEM) determined particle size and shape based on measurements from at least 100 particles (Central Research Facility, IIT Delhi) (JEOL JEM-2100F). Zeta potential measurements assessed surface charge and colloidal stability, while the point of zero charge (pH_{pzc}) was established using the pH drift method (Nanoscale Research Facility, IIT Delhi). Fourier transform infrared spectroscopy (FTIR) in the range of 400–4000 cm^{-1} identified functional groups and surface interactions between tea tree oil components and iron oxide (Department of Physics and Material Sciences, JIIT Noida). X-ray diffraction (XRD) with Cu Kα radiation (λ = 1.5406 Å) over a 2θ range of 10–80° was used to analyse crystalline structure and phase composition (Department of Physics and Material Sciences, JIIT, Noida). Gas chromatography–mass spectrometry (GC–MS) identified the major phytochemical constituents of tea tree oil responsible for nanoparticle stabilization (Advanced Instrumentation Research Facility, JNU) (Shimadzu QP-2010 Plus with Thermal Desorption System TD 20).

3.1 Sample Characterizations

3.1.1 FESEM (Field-Emission Scanning Electron Microscopy)

Field-emission scanning electron microscopy (FESEM) images showed that the formed iron oxide nanoparticles were irregularly shaped, moderately clumped, and rough. The particles were grouped as small aggregates rather than large crystals, suggesting that nucleation during the tea tree oil-mediated synthesis was successful. The clumping is likely due to magnetic dipole-dipole interactions and high surface energy, both typical of nanosized iron oxides. Even though the particles are aggregated, the lack of dense microcrystalline blocks confirms they are at the nanoscale. This type of structure is often seen in green-synthesized iron oxide nanoparticles. In these cases, phytochemical capping slows down particle growth but does not fully stop magnetic aggregation [3, 7].

Energy-dispersive X-ray spectroscopy (EDS) elemental mapping showed that iron (Fe) and oxygen (O) were present and evenly distributed across the nanoparticle surface, indicating that iron oxide had formed successfully. The even distribution of Fe and O signals indicates consistent oxide formation rather than separate metallic clusters. Carbon (C) detected in the spectrum likely

comes from organic compounds on the surface, which are from tea tree oil used as stabilizers. This observation strongly supports the proposed green synthesis mechanism, where bioactive compounds present in tea tree oil facilitate the reduction of iron precursors while simultaneously stabilizing the nanoparticles through surface functionalization. The rough, uneven surfaces observed in FESEM micrographs indicate greater surface area and a higher number of exposed Fe–OH groups. These features are important for arsenate adsorption through inner-sphere complexation. Surface defects and irregular textures increase the number of active sites and enhance adsorption efficiency, as reported for iron oxide-based adsorbents [3, 4, 8,9]. The FESEM results for iron oxide nanoparticles derived from essential oil are well depicted in Figure 1, showing the morphology in Figure 1(a), EDS elemental mapping in Figure 1(b), and the EDS spectrum in Figure 1(c).

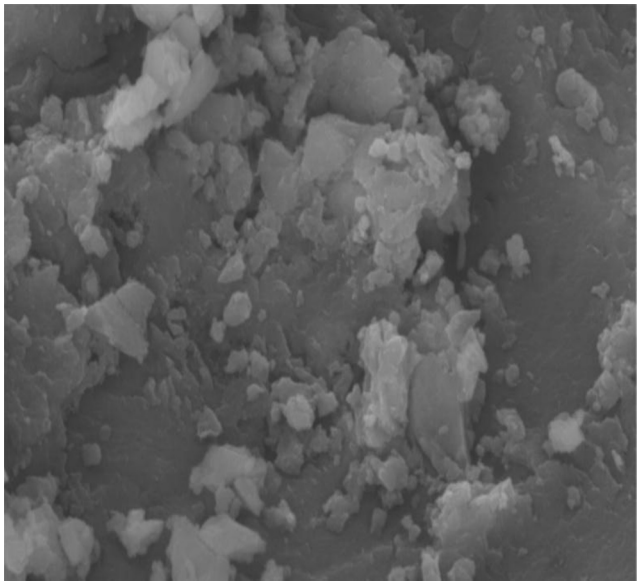

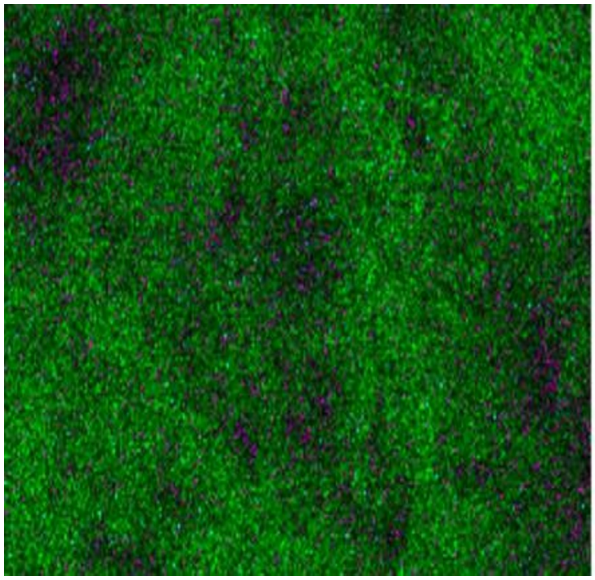

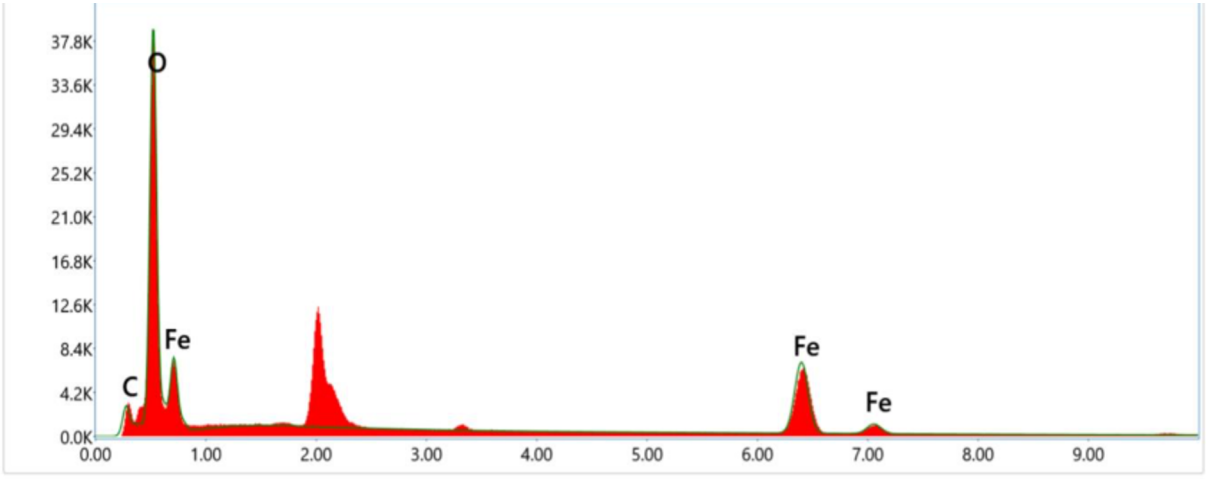

Det: Octane Elite Super

eZAF Quant Result - Analysis Uncertainty: 99.00 %

Element	Weight %	Atomic %	Error %
C K	12.8	23.2	11.0
O K	44.2	60.1	7.8
Fe K	42.9	16.7	2.9

Fig. 1 (a)FESEM image of Essential oil derived Iron oxide nanoparticles

(b) EDS elemental mapping illustrating the uniform distribution of Fe, O, and C elements

(c) EDS spectrum along with quantitative elemental composition confirming the presence of Fe, O, and C.

Figure 1. (a) FESEM, (b) and (c) EDS and elemental mapping images of Essential oil derived Iron oxide Nanoparticles.

3.1.2 TEM (Transmission Electron Microscopy)

TEM images showed that nanoscale iron oxide particles formed with shapes ranging from almost round to irregular. Most nanocrystallites measured 15–30 nm, while larger structures were loosely clustered, likely due to magnetic dipole interactions. The darker, denser areas in the images point to iron-rich regions, confirming that nanoparticles formed successfully. This kind of aggregation is typical of iron oxide nanoparticles due to their high surface energy and magnetic properties. These shapes and sizes match those reported for green-synthesized Fe_3O_4 nanoparticles, which typically range from 10 to 40 nm and exhibit some clustering [10, 7]. The nanoscale particle size observed (about 15–30 nm) increases the surface-to-volume ratio and increases the number of exposed surface hydroxyl groups (≡Fe–OH). This helps arsenate bind more efficiently through inner-sphere surface complexation. Smaller particles also lower diffusion barriers, which leads to faster adsorption. Previous studies have also found that smaller iron oxide particles improve arsenate adsorption [4, 10].

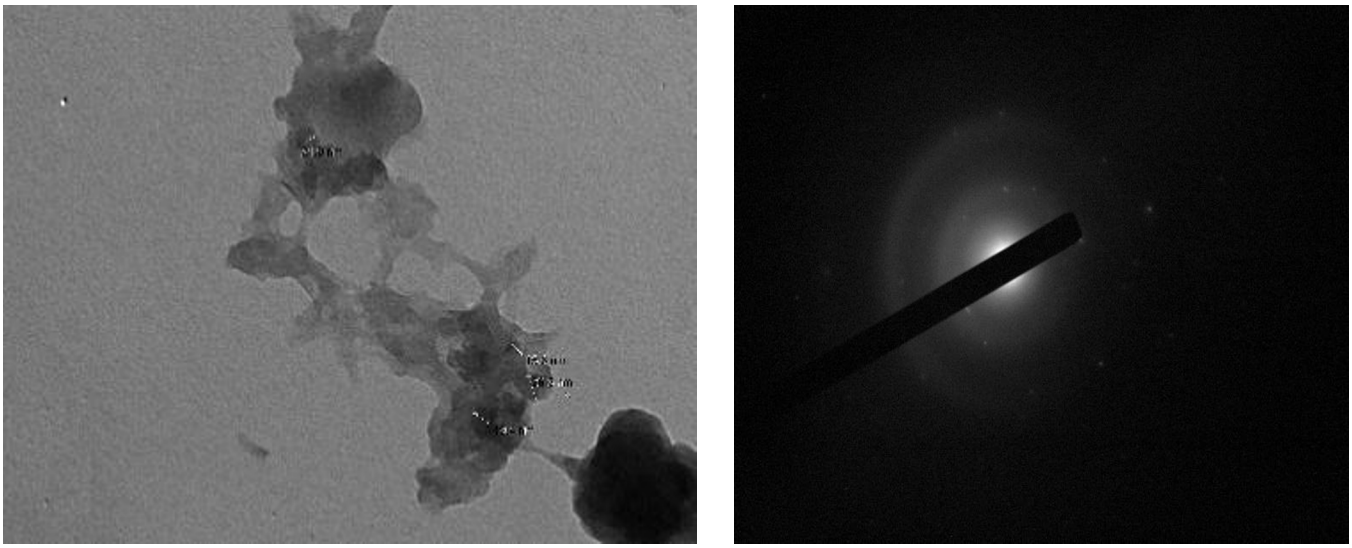

Figure 2. (a) and (b) TEM images of Essential oil derived Iron oxide Nanoparticles.

3.1.3 FTIR (Fourier Transform Infrared Spectroscopy)

The FTIR spectrum of tea tree oil-mediated iron oxide nanoparticles showed a broad absorption band at 3331 cm^{-1}, which matches O–H stretching vibrations from surface hydroxyl groups and alcohols in tea tree oil. The peak at 1634 cm^{-1} is linked to C=O or C=C stretching vibrations, suggesting oxygenated monoterpenes are present on the nanoparticle surface. The absorption band at 1073 cm^{-1} corresponds to Fe–O stretching vibrations, confirming the formation of iron oxide nanoparticles. The combination of organic functional groups and the Fe–O band indicates that phytochemicals helped reduce and stabilize the iron oxide nanoparticles. These results match previous FTIR studies of green-synthesized iron oxide nanoparticles, where Fe–O vibrations are usually found between 500 and 1100 cm^{-1}, and surface hydroxyl bands appear around 3200 to 3400 cm^{-1} [3, 7].

Figure 3. FTIR of Essential oil derived Iron oxide Nanoparticles.

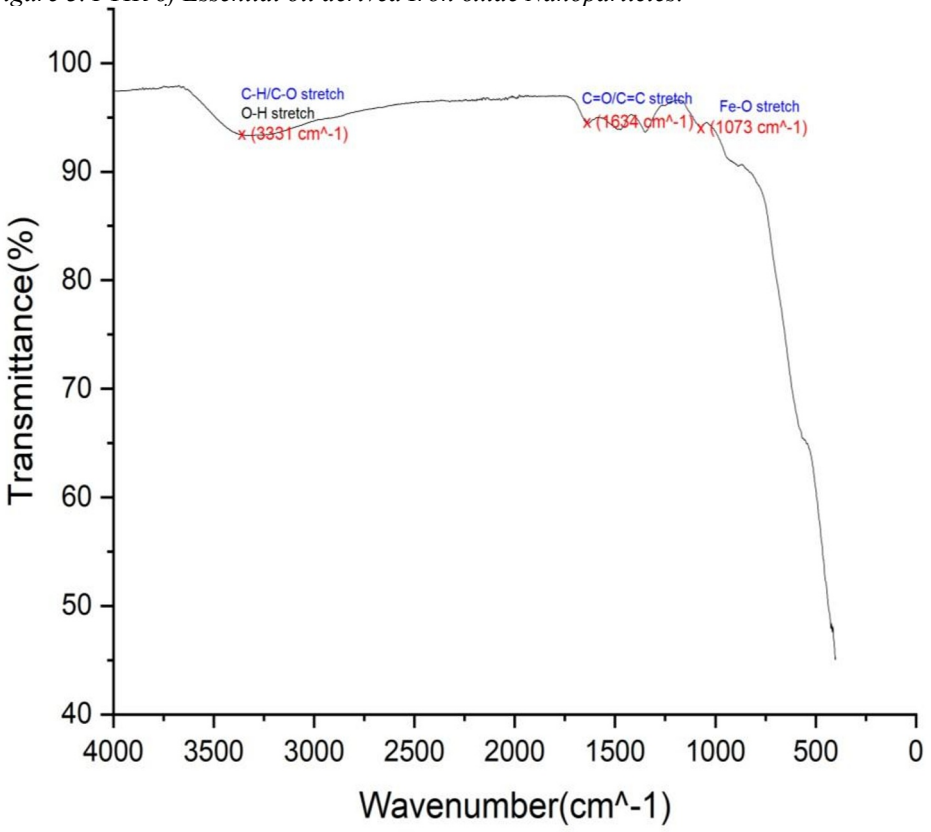

3.1.4 XRD (X-Ray Diffraction)

The XRD pattern showed diffraction peaks at 2θ = 14.76°, 33.94°, 58.26°, and 79.72°, indicating the crystalline nature of the synthesized nanoparticles. The reflections in the higher 2θ region (≈33.94°, 58° and 79°) are characteristic of iron oxide crystalline planes, confirming nanoparticle formation. However, the peak at 2θ = 14.76° does not correspond to standard reflections of magnetite (Fe_3O_4) or maghemite (γ-Fe_2O_3) and is therefore attributed to the presence of organic compounds derived from tea tree oil. This low-angle peak likely arises from amorphous or semicrystalline phytochemical residues that act as capping and stabilizing agents on the nanoparticle surface. The relatively broad and low-intensity peaks suggest nanoscale crystallite size and partial amorphous contribution from organic capping layers of tea tree oil. In iron oxide systems, characteristic reflections for magnetite (Fe_3O_4) or maghemite (γ-Fe_2O_3) commonly appear in the range of 30–65° (2θ) using Cu Kα radiation, and peak broadening is typically associated with nanosized crystallites [3, 11]. Identification of crystalline iron oxide phases and an amorphous organic layer supports the proposed green synthesis mechanism, where phytochemicals from tea tree oil facilitate the reduction of iron precursors while simultaneously stabilizing the nanoparticles. reveals structured Fe–O lattices that can provide surface hydroxyl groups (≡Fe–OH) needed for arsenate binding via inner-sphere complexation. Crystallinity and nanoscale peak broadening are also associated with a larger surface area and improved adsorption performance [3, 4].

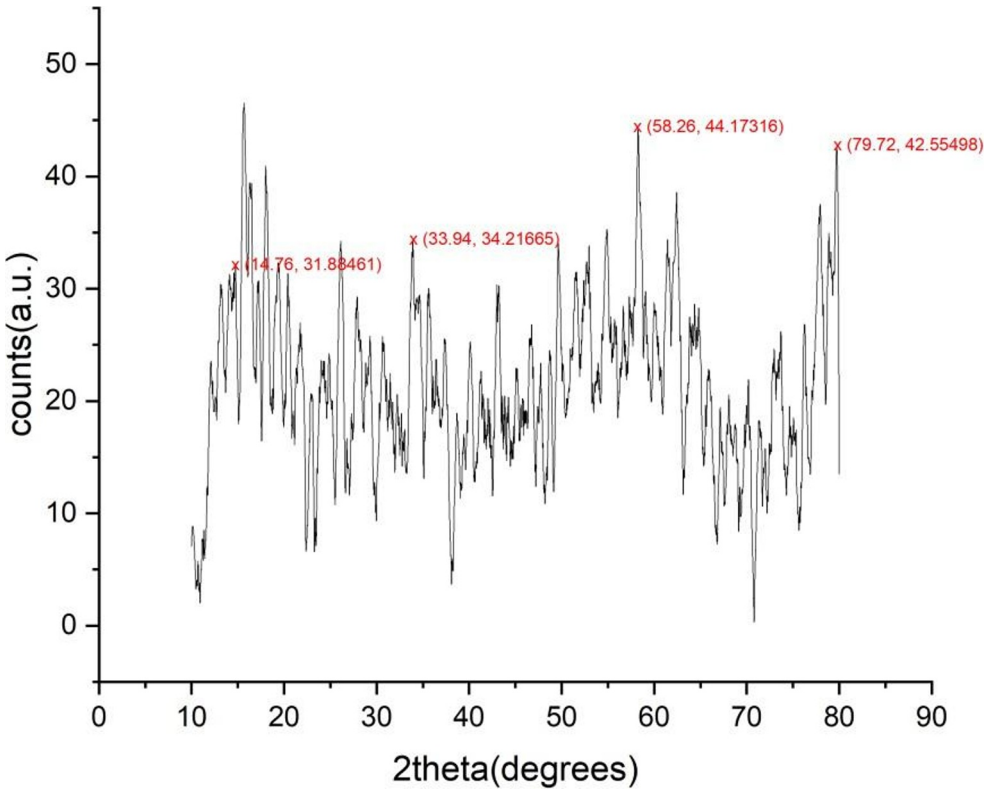

Figure 4. XRD of essential oil-derived iron oxide Nanoparticles.

3.1.5 GC–MS (Gas Chromatography–Mass Spectrometry)

GC–MS analysis identified 22 components that accounted for the entire chromatographic area. The main compound was terpinen-4-ol (RT 16.104 min, 55.23%), indicating a terpinen-4-ol–rich composition of the tea tree oil. Although this value is higher than the commonly reported 30–48% range for *Melaleuca alternifolia* essential oil [12,13], such variation is well known and can arise from differences in plant origin, environmental conditions, extraction methods, and storage. Higher terpinen-4-ol content is often associated with improved bioactivity and stronger reducing potential. Other major components were γ-terpinene (5.72%), p-cymene (3.91%), and bicyclic monoterpene derivatives (about 5%), which are typical monoterpene hydrocarbons found in tea tree oil [13]. Oxygenated monoterpenes like α-terpineol (2.61%) and linalool (0.79%) were also present. The high amount of hydroxyl-containing monoterpenes suggests they help both reduce and stabilize iron oxide nanoparticles, supporting surface coordination and stabilization [12].

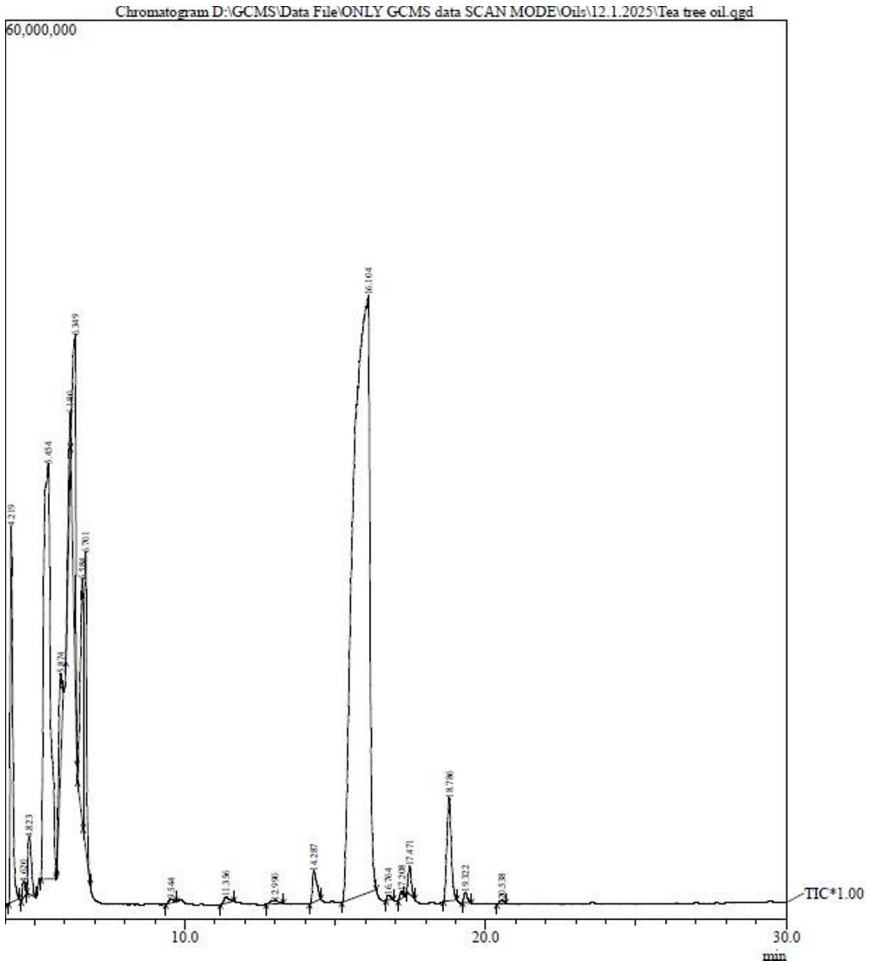

Figure 5. GC-MS of Essential oil derived Iron oxide Nanoparticles.

3.1.6 Zeta Potential

The iron oxide nanoparticles prepared with tea tree oil exhibited a zeta potential of −20.0 mV, suggesting moderate colloidal stability. Zeta potential values around ±20 mV are usually enough to provide electrostatic stabilization in nanoparticle dispersions [14]. The negative surface charge likely arises from deprotonated surface hydroxyl groups (≡Fe–O⁻) and from oxygenated monoterpenes in tea tree oil, especially terpinen-4-ol and α-terpineol. Other studies have reported similar zeta potential values (−18 to −25 mV) for iron oxide nanoparticles prepared using green methods, in which phytochemicals on the surface help stabilize the particles [9, 8]. Zeta potential analysis helps us understand the surface charge of iron oxide nanoparticles, which affects their interactions with arsenate. The negative surface potential shows that deprotonated surface hydroxyl groups (≡Fe–O⁻) are present. These groups control arsenate adsorption at different pH values through electrostatic attraction and by forming inner-sphere complexes with As(V) oxyanions [4, 14].

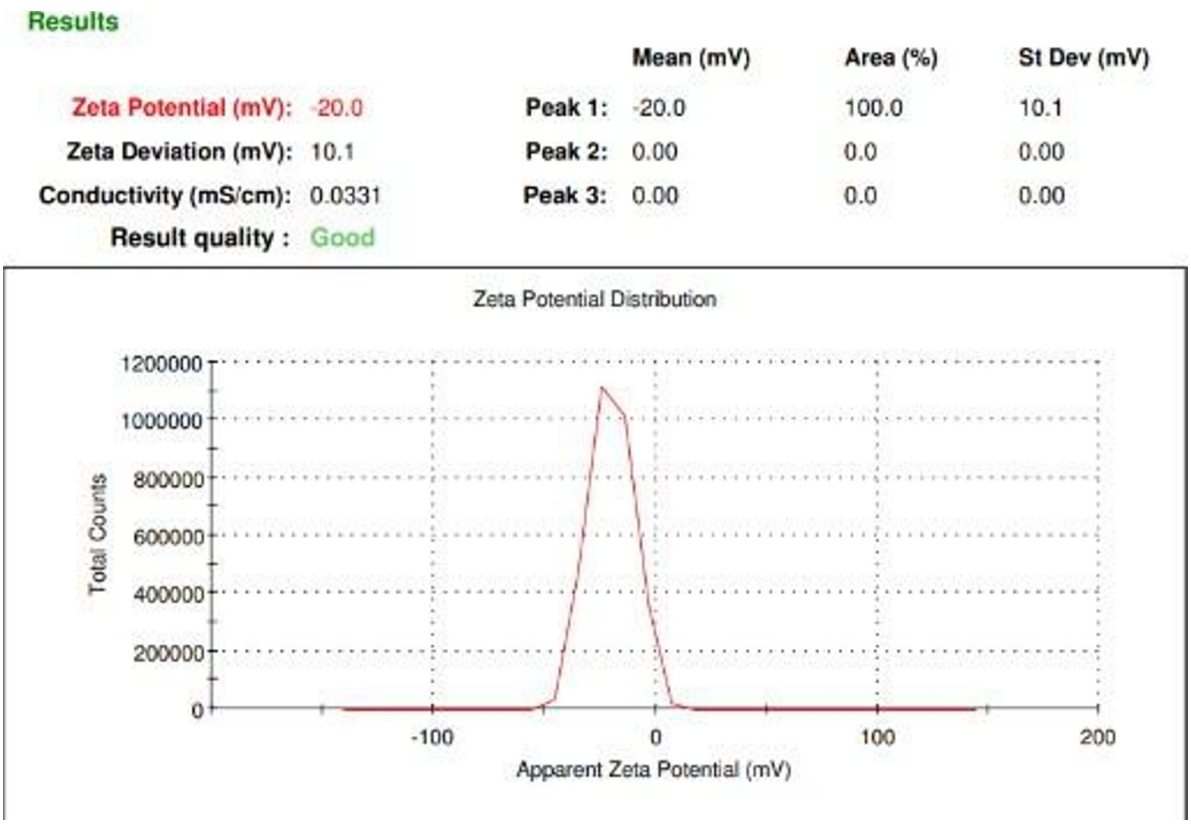

Figure 6. Zeta Potential of Essential oil derived Iron oxide Nanoparticles.

4. Batch Experiment for As(V) Removal

4.1 Batch Adsorption Experiments

We conducted batch adsorption studies to assess the effectiveness of iron oxide nanoparticles in removing As(V). Experimental Conditions: Volume of arsenic solution: 50 mL, Adsorbent dose: 50 mg, Temperature: Ambient temperature, Agitation: Constant shaking, Pressure: Atmospheric, Contact time: 15–240 min, Equilibrium time: 240 min.

Adsorption capacity was calculated using:

$$qt = \frac{(Co - Ct) \times V}{m}$$

Since, V = 0.05L and m = 0.05g, the equation simplifies to: **qt= (Co- Ct)**

Removal Efficiency was calculated by: $\text{Removal \%} = \frac{(Co - Ct) \times 100}{Co}$

4.1.1 Effect of pH

The ability of iron-oxide adsorbents to remove arsenate (As(V)) depends a lot on pH, since both the form of arsenate in water and the surface charge of iron oxides change with pH. In oxidizing conditions, arsenate is mainly found as $H_2AsO_4^-$ and $HAsO_4^{2-}$. Between about pH 2 and 7, $H_2AsO_4^-$ is the main form, and it binds well to the positively charged Fe–OH sites on iron oxides through inner-sphere complexation. As a result, adsorption is usually highest in the acidic to near-neutral range (often around pH 4 to 6) and drops off at higher pH, when the surface charge becomes less positive or even negative, leading to more electrostatic repulsion. This trend has been seen in studies on hydrous ferric oxides and iron-oxide minerals and is discussed in important reviews and experiments [4, 15]. More recent work on Fe-based adsorbents also shows the best As(V) uptake at pH 4–6 [16, 17]. In the experiments, the highest removal at pH 5 ($q_e \approx 9.68$ mg·g^{-1} at 10 ppm; 47.9 mg·g^{-1} at 50 ppm; 94.6 mg·g^{-1} at 100 ppm) fits this well-known pattern and supports inner-sphere complexation as the main uptake mechanism.

4.1.2 Effect of Concentration

When you change the initial arsenate concentration while keeping the adsorbent dose, pH, and volume constant, you can directly measure the adsorbent's working capacity (q_e) and observe how the adsorption isotherm looks. At higher starting concentrations, the concentration difference is larger, so more arsenate moves onto the adsorbent, and q_e increases. However, the percentage removed may stay about the same or drop a bit if there are not enough surface sites left. This pattern is common in arsenate adsorption studies and is why researchers use different starting concentrations to build Langmuir or Freundlich isotherms and estimate q_{max} and affinity constants, as shown in many studies. The results q_e increasing with higher starting concentrations (about 9.68, 47.9, and 94.6 mg·g^{-1} for 10, 50, and 100 ppm at pH 5) and high removal rates (around 95% at 50 and 100 ppm after 240 minutes) match what is usually seen with Fe-based adsorbents. This supports the use of the 5–100 ppm calibration range, which is common in adsorption research [18].

4.2 Adsorption Kinetics

Adsorption kinetics explain how quickly a solute is removed from water and help us understand what controls the adsorption process. Kinetic models show if adsorption happens through physical sorption, chemisorption, or is limited by diffusion. Two common models are the pseudo-first-order (PFO) model by Lagergren and the pseudo-second-order (PSO) model by Ho and McKay. The PFO model states that the rate depends on the number of adsorption sites still available, whereas the PSO model suggests that chemisorption, which involves valence forces or electron sharing, is the main factor [19, 20].

Batch experiments were conducted at the optimum pH of 5 using an initial arsenate concentration of 10 ppm. The equilibrium adsorption capacity obtained experimentally was:

$$q_e(exp) = 9.68 mg\ g{-}1$$

Pseudo- First Order Model:

$\ln(q_e - q_t) = \ln q_e - k_1 t$ where:

- q_t= adsorption capacity at time t
- q_e= equilibrium adsorption capacity
- k_1= pseudo-first-order rate constant (min^{-1})

A linear relationship was found, but the correlation coefficient (R^2) was lower than that of the pseudo-second-order model. The calculated q_e also differed from the experimental value. This means the PFO model does not accurately describe the adsorption mechanism.

Pseudo- Second Order Model:

$t/q_t = (1/k_2 q_e^2) + (t/q_e)$

where:

- k_2= pseudo-second-order rate constant (g mg^{-1} min^{-1})

The calculated q_e from the PSO model (9.73 mg g^{-1}) was very close to the experimental value (9.68 mg g^{-1}). This shows that As(V) adsorption onto iron oxide nanoparticles follows pseudo-second-order kinetics. This suggests that chemisorption, in which arsenate species ($H_2AsO_4^-$) form surface complexes with Fe–OH sites, is the rate-limiting step. Such kinetic behaviour has been widely reported for arsenate adsorption onto iron-based adsorbents [20, 4].

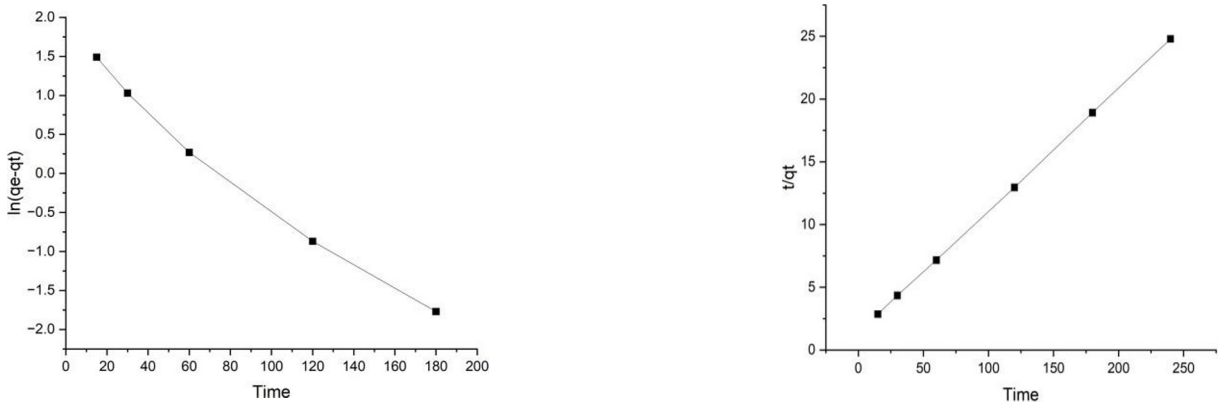

Figure 7. (a) Pseudo-First-Order Model, and (b) Pseudo-Second-Order Model at pH 5 for an initial concentration of 10 ppm.

Table 1: Kinetic adsorption parameters for As(V) adsorption

Parameter	Pseudo-First-Order	Pseudo-Second-Order
q_e(exp)	9.68	9.68
q_e(cal)	6.30	9.73
k	0.0204	0.0086
R^2	0.95	0.998
h	–	0.81

4.3 Adsorption Isotherm

Adsorption isotherms show how the concentration of a substance in a solution relates to the amount that adsorbs to a solid surface at a given temperature. These models help us understand how much can be adsorbed, how even the surface is, and how the process works. The two isotherm models used most often are: Langmuir isotherm, which assumes monolayer adsorption onto a homogeneous surface with a finite number of identical sites; and Freundlich isotherm, which describes adsorption on non-uniform surfaces and allows for multiple adsorption layers [21, 22].

Langmuir Isotherm:

$Ce/qe = (1/q^{b}) +$

$(Ce/qmax)$

where:

- C_e= equilibrium concentration (ppm)
- q_e= adsorption capacity (mg g^{-1})
- q_{max}= maximum monolayer adsorption capacity
- b= Langmuir affinity constant

Equilibrium data at pH 5 after 240 minutes, using initial concentrations of 10, 50, and 100 ppm, were used for isotherm modeling. The Langmuir plot (Ce/qe vs. Ce) was highly linear, confirming that the monolayer adsorption model fits well. Linear regression of the Langmuir equation gave these

parameters: Maximum adsorption capacity, q_{max} = 216.9 mg g−1, Langmuir affinity constant, b = 0.149 L mg−1

The high qmax value shows that iron oxide nanoparticles have a strong adsorption capacity for As(V). This is similar to or better than many Fe-based adsorbents reported in earlier studies **[4, 15].**

The dimensionless separation factor (RL) was calculated using:

$$RL = 1/\ 1+ bC_o$$

Because all R_l values are between 0 and 1, the adsorption process is favorable for the concentration range studied. When R_l is between 0 and 1, adsorption is favorable; R_l equal to 1 means the process is linear; R_l greater than 1 means it is unfavorable; and R_l equal to 0 means the process is irreversible. Overall, the good linearity of the Langmuir model and the high q_{max} value suggest that As(V) forms a monolayer on homogeneous Fe–OH active sites of the iron oxide nanoparticles. This behavior is commonly observed in arsenate adsorption on iron oxides [21].

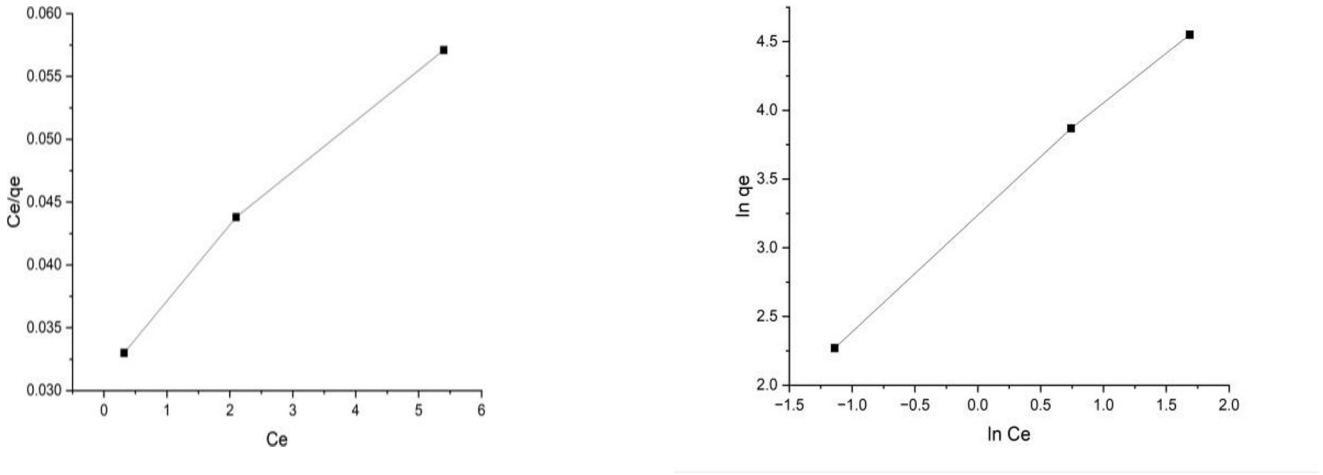

Figure 8. (a) Langmuir plot, and (b) Freundlich plot for As(V) removal onto iron oxide nanoparticles at pH 5 (240 min, 50 mg adsorbent dose, 50 mL solution, ambient temperature).

Table 2: Langmuir and Freundlich model parameters.

Parameter	Langmuir	Freundlich
q_{max} (mg g^{-1})	216.9	–
b (L mg^{-1})	0.149	–
Kf	–	22.6
n	–	1.32
R^2	0.998	0.987

Freundlich Isotherm:

$$\ln q_e = \ln K_f + (1/n)$$

$$\ln C_e$$ where:

- K_f= adsorption capacity constant
- n= adsorption intensity parameter

The Freundlich isotherm constants were determined from a linear plot of ln q_e versus ln C_e. The calculated values were Kf = 22.6 and n = 1.32. Because n is greater than 1, the adsorption of As(V) onto iron oxide nanoparticles is considered favorable.

However, comparing the correlation coefficients showed that the Langmuir model fit the data better, suggesting that adsorption occurs mainly as a monolayer [22, 23, 4].

4.4 Proposal of Mechanism

Based on pH-dependent adsorption behavior, kinetic modelling, and isotherm analysis, the removal of As(V) by iron oxide nanoparticles is proposed to occur predominantly via inner-sphere surface complexation. Maximum adsorption at pH 5 corresponds to the predominance of $H_2AsO_4^-$ species and the positively charged $Fe–OH_2^+$ surface sites under mildly acidic conditions, promoting strong electrostatic attraction followed by ligand exchange. The excellent fit to the pseudo-second-order model ($R^2 \approx 0.998$) and close agreement between experimental and calculated q_e values indicate that chemisorption is the rate-limiting step. Furthermore, the Langmuir isotherm provided superior linearity ($R^2 \approx 0.998$) with a high maximum adsorption capacity ($q_{ma}^x = 216.9$ mg g^{-1}), suggesting monolayer adsorption on homogeneous Fe–OH active sites. These observations collectively support a surface complexation mechanism involving Fe–O–As bond formation, consistent with established reports for arsenate adsorption on iron oxides [4]. However, this investigation represents a preliminary batch adsorption study, and further work is required to fully elucidate the adsorption mechanism and the system's practical applicability. Further support for the proposed mechanism is provided by Hu et al. (2023) and Wang et al. (2022), who strongly corroborate that As(V) adsorption on iron-based nanomaterials is predominantly governed by inner-sphere surface complexation involving ligand exchange with surface Fe–OH groups.

5. Conclusion and Discussion

This study shows that iron oxide nanoparticles can be synthesized in an environmentally friendly way using tea tree oil as a reducing and stabilizing agent. These nanoparticles were tested for their ability to remove arsenate [As(V)] from water. The experiments found that arsenate removal effectiveness depended strongly on solution pH, with the best results at pH 5. This matches the presence of $H_2AsO_4^-$ species in mildly acidic conditions and the positive charge on the nanoparticle surfaces, which helps attract arsenate. Most of the arsenate was removed quickly in the first 60 minutes, and the rate slowed as it approached equilibrium at around 240 minutes, suggesting that surface active sites were gradually filled.

The kinetic analysis found that the pseudo-second-order (PSO) model matched the data very well ($R^2 \approx 0.998$), and the calculated and experimental q_e values were very close. This suggests that chemisorption is the main rate-controlling process. The Langmuir isotherm model also fit the data better than the Freundlich model, showing that arsenate forms a single layer on similar active sites. The nanoparticles exhibited a high maximum adsorption capacity ($q_{ma}^x = 216.9$ mg g^{-1}), indicating strong attraction to arsenate. Both the separation factor ($0 < R_l < 1$) and the Freundlich constant ($n > 1$) indicate that adsorption was favorable across the tested concentrations. The main mechanism of As(V) adsorption appears to be inner-sphere surface complexation, in which arsenate exchanges with surface ≡Fe–OH groups. This process is helped by electrostatic interactions at the best pH. Compounds in tea tree oil may also alter the surface and increase the number of active sites, thereby improving the adsorption of arsenate by nanoparticles. It is important to note that this study is an early investigation done in controlled lab conditions. More research is needed to fully understand how adsorption works and how the material can be used in practice. Future work should examine thermodynamic analysis, intraparticle diffusion, surface changes after adsorption (e.g., via XPS), the material's reusability, and its performance in real water containing other ions. These studies will help clarify the process and determine whether the material is suitable for large-scale arsenic removal.

References

1. WHO (2017). Guidelines for Drinking-water Quality, 4th ed., incorporating 1st addendum. World Health Organization.
2. Smedley, P.L., Kinniburgh, D.G. (2002). A review of the source, behaviour and distribution of arsenic in natural waters. Applied Geochemistry, 17, 517–568.
3. Cornell, R.M., Schwertmann, U. (2003). The Iron Oxides. Wiley-VCH.
4. Dixit, S., Hering, J.G. (2003). Comparison of arsenic(V) and arsenic(III) sorption onto iron oxide minerals. Environmental Science & Technology, 37, 4182–4189.
5. Laurent, S. et al. (2008). Magnetic iron oxide nanoparticles: synthesis, stabilization, vectorization. Chemical Reviews, 108, 2064–2110.
6. Borotová, P. et al. (2022). Chemical composition and bioactivity of tea tree oil. Molecules, 27, 558.

7. Mohapatra, J., et al. (2015). Green synthesis of Fe_3O_4 nanoparticles and their characterization. Applied Surface Science, 346, 608–615.
8. Salem, S.S., Fouda, A., et al. (2019). Green synthesis of metal and metal oxide nanoparticles and their biomedical applications. Applied Surface Science, 463, 825–834.
9. Feng, B., Hong, R.Y., Wang, L.S., Guo, L., Li, H.Z., Ding, J., Zheng, Y. (2012). Synthesis of Fe_3O_4 nanoparticles and their magnetic properties. Journal of Hazardous Materials, 217–218, 439–446.
10. Gupta, A.K., & Gupta, M. (2005). Synthesis and surface engineering of iron oxide nanoparticles for biomedical applications. Biomaterials, 26(18), 3995–4021.
11. Cullity, B.D., & Stock, S.R. (2001). Elements of X-Ray Diffraction (3rd ed.). Prentice Hall, Upper Saddle River, NJ.
12. Carson, C.F., Hammer, K.A., & Riley, T.V. (2006). Melaleuca alternifolia (Tea Tree) oil: a review of antimicrobial and other medicinal properties. Clinical Microbiology Reviews, 19(1), 50–62.
13. Brophy, J.J., Davies, N.W., Southwell, I.A., Stiff, I.A., & Williams, L.R. (1989). Gas chromatographic quality control for oil of Melaleuca terpinen-4-ol type (Australian tea tree). Journal of Agricultural and Food Chemistry, 37(5), 1330–1335.
14. Bhattacharjee, S. (2016). DLS and zeta potential – What they are and what they are not? Journal of Controlled Release, 235, 337–351.
15. Bissen, M., & Frimmel, F.H. (2003). Arsenic – a review. Part I: Occurrence, toxicity, speciation, mobility. Acta Hydrochimica et Hydrobiologica, 31(1), 9–18.
16. Liu, Y., Ma, J., Liu, X., & Liu, X. (2010). Adsorption of arsenate from aqueous solution by Fe–Mn binary oxide. Journal of Hazardous Materials, 173, 377–383.
17. Aredes, S., Klein, B., & Pawlik, M. (2012). The removal of arsenic from water using natural iron oxide minerals. Journal of Cleaner Production, 29–30, 208–213.
18. Rahman, M.A., Hasegawa, H., Rahman, M.M., Rahman, M.A., & Miah, M.A.M. (2022). Arsenic accumulation in rice and mitigation strategies: A review. Chemosphere, 287, 132187.
19. Lagergren, S. (1898). Zur Theorie der sogenannten Adsorption gelöster Stoffe. Kongliga Svenska Vetenskapsakademiens Handlingar, 24, 1–39.
20. Ho, Y.S., & McKay, G. (1999). Pseudo-second order model for sorption processes. Process Biochemistry, 34(5), 451–465.
21. Langmuir, I. (1918). The adsorption of gases on plane surfaces of glass, mica and platinum. Journal of the American Chemical Society, 40(9), 1361–1403.
22. Freundlich, H.M.F. (1906). Über die Adsorption in Lösungen. Zeitschrift für Physikalische Chemie, 57, 385–470.
23. Foo, K.Y., & Hameed, B.H. (2010). Insights into the modeling of adsorption isotherm systems. Chemical Engineering Journal, 156(1), 2–10.
24. Wang, Yulong, et al. "Arsenic removal performance and mechanism from water on iron hydroxide nanopetalines." *Scientific Reports* 12.1 (2022): 17264.
25. Hu, Shan, Huanhuan Fu, and Jingyi Fu. "Distinct effects of Fe3+ on the adsorption of chromate and arsenate: A comparison of iron-bearing ferrihydrite and nano-TiO2 absorbents." *Environmental Technology & Innovation* 32 (2023): 103418.